

Synthesis, Structure, and Spectroscopic Properties of Perhexyloligosilanes

Kuninori Obata[†] and Mitsuo Kira^{*,†,‡}

Photodynamics Research Center, The Institute of Physical and Chemical Research (RIKEN), 19-1399 Koeji, Nagamachi, Aoba-ku, Sendai 980-0868, Japan, and Department of Chemistry, Graduate School of Science, Tohoku University, Aoba-ku, Sendai, 980-8578, Japan

Received January 4, 1999

A series of linear perhexyloligosilanes (Hex(SiHex₂)_nHex, $n = 3-10$) was prepared by Wurtz coupling of a mixture of trihexylchlorosilane and dihexyldichlorosilane. The $\sigma \rightarrow \sigma^*$ absorption maxima red-shift with increasing chain length, which is similar to what was observed for a series of permethyloligosilanes. However, the temperature dependence of the spectra is significantly different between these two series. The origin of the blue shift with decrease in temperature observed for short-chain oligosilanes ($n = 3-5$) is ascribed to the parabolic dependence of the transition energies on the SiSiSi bond angle. The red shift of the absorption maxima observed for long-chain oligosilanes ($n = 6-10$) probably results from the ordering of the chain to the all pseudo-trans (extended) form at low temperatures. The long-chain perhexyloligosilanes show stronger temperature dependence similar to that of perhexylpolysilane polymers, suggesting that the barriers of the transition from the folded to extended chains are much larger than those for permethyloligosilanes, due to the steric effects of the side-chain alkyl substituents. The emission spectral features of perhexyloligosilanes are essentially similar to those of permethyloligosilanes studied by Michl et al. A significant difference between these two series of oligosilanes is also observed on the temperature dependence of the emission spectra.

Introduction

Much attention has been focused on linear-chain polysilane polymers, whose main chains are constructed by Si–Si bonds, because of their unique optoelectronic properties.¹ Typically, while poly(dihexylsilylene) exhibits an intense absorption band at 315 nm at room temperature, upon cooling below ca. -30 °C, the absorption bandwidth becomes much narrower and the maximum shifts to 355 nm.² The origin of the thermochromism is usually ascribed to the transition at low temperatures from a random coil to a pseudo-trans rod of the silicon backbone,^{2,3} while Miller et al. have proposed that the red shift with decreasing temperature is caused by aggregation of polysilane chains.⁴ Due to the high molecular weights of polysilanes and their dispersion, it is very difficult to investigate the relation-

ship between the main-chain conformation and optical properties in detail. Studies of linear oligosilanes having discrete molecular weights as models for polysilanes are highly desirable. About four decades ago, as pioneering studies in this field, Wilson, Kumada, and Gilman and their co-workers reported the synthesis and characterization of a series of linear permethyloligosilanes.⁵ Their absorption maxima at room temperatures were found to red-shift upon increasing the number of silicon atoms in the chain and assigned to the $\sigma \rightarrow \sigma^*$ transitions.⁶ During the course of our studies, Michl et al. have reported⁷ detailed studies of the photophysics of per-

[†] The Institute of Physical and Chemical Research (RIKEN).

[‡] Tohoku University.

(1) For reviews, see: (a) Miller, R. D.; Michl, J. *Chem. Rev.* **1989**, *89*, 1359. (b) Michl, J.; Downing, J. W.; Karatsu, T.; McKinley, A. J.; Poggi, G.; Wallraff, G. M.; Sooriyakumaran, R.; Miller, R. D. *Pure Appl. Chem.* **1988**, *60*, 959. (c) Zeigler, J. M. *Synth. Met.* **1989**, *28*, C581. (d) West, R. *J. Organomet. Chem.* **1986**, *300*, 327. (e) West, R. In *The Chemistry of Organosilicon Compounds*; Patai, S., Rappoport, Z., Eds.; J. Wiley and Sons: Chichester, 1989; Chapter 19, p 1207. (f) Kira, M.; Miyazawa. In *The Chemistry of Organosilicon Compounds Vol. 2*; Rappoport, Z., Apeloig, Y., Eds.; J. Wiley and Sons: Chichester, 1998; Chapter 22, p 1311.

(2) (a) Harrah, L. A.; Zeigler, J. M. *J. Polym. Sci.: Polym. Lett. Ed.* **1985**, *23*, 209. (b) Trefonas, P.; Danewood, J. R., Jr.; West, R.; Miller, R. D. *Organometallics* **1985**, *4*, 1318.

(3) Our recent study has suggested that a poly(dihexylsilylene) molecule has several loose helical (pseudo-trans) segments with kinks at low temperatures in solution: Obata, K.; Kira, M. *Macromolecules* **1998**, *31*, 4666, and references therein.

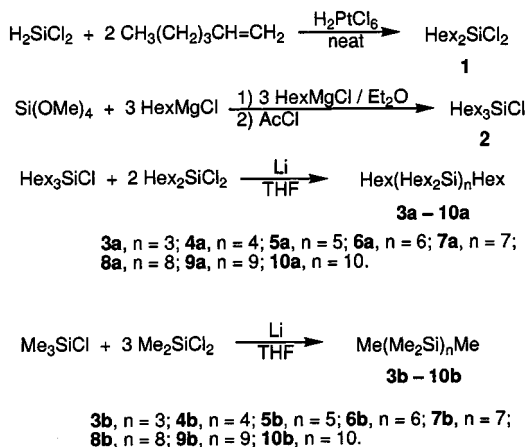
(4) (a) Miller, R. D.; Wallraff, G. M.; Baier, M.; Cotts, P. M.; Shukla, P.; Russell, T. P.; De Schryver, F. C.; Declercq, D. *J. Inorg. Organomet. Polym.* **1991**, *1*, 505. (b) Shukla, P.; Cotts, P. M.; Miller, R. D.; Russell, T. P.; Smith, B. A.; Wallraff, G. M.; Baier, M.; Thiagarajan, P. *Macromolecules* **1991**, *24*, 5606.

(5) (a) Wilson, G. R.; Smith, A. G. *J. Org. Chem.* **1961**, *26*, 557. (b) Kumada, M.; Ishikawa, M. *J. Organomet. Chem.* **1963**, *1*, 153. (c) Kumada, M.; Ishikawa, M.; Maeda, S. *J. Organomet. Chem.* **1966**, *5*, 120. (d) Kumada, M.; Tamao, K. *Adv. Organomet. Chem.* **1968**, *6*, 19. (e) Gilman, H.; Atwell, W. H.; Schwabke, G. L. *Chem. Ind. (London)* **1964**, 1063. (f) Gilman, H.; Atwell, W. H.; Schwabke, G. L. *J. Organomet. Chem.* **1964**, *2*, 369. (g) Gilman, H.; R. L. Harrell, T. *J. Organomet. Chem.* **1966**, *5*, 201. (h) Boberski, W. G.; Allred, A. L. *J. Organomet. Chem.* **1975**, *88*, 65.

(6) (a) Shorygin, P. P.; Petakhov, V. A.; Nefedov, O. M.; Kolesnikov, S. P.; Shiryaev, V. I. *Theor. i Eksperim. Khim. Akad. Nauk Ukr. SSR* **1966**, *2*, 190. (b) Pitt, C. G.; Bursay, M. M.; Rogerson, P. F. *J. Am. Chem. Soc.* **1970**, *92*, 519. (c) Ramsey, B. G. *Electronic Transitions in Organometallics*; Academic Press: New York, 1968.

(7) (a) Balaji, V.; Michl, J. *Polyhedron* **1991**, *10*, 1265. (b) Sun, Y.-P.; Michl, J. *J. Am. Chem. Soc.* **1992**, *114*, 8186. (c) Sun, Y.-P.; Hamada, Y.; Huang, L.-M.; Maxka, J.; Hsiao, J.-S.; West, R.; Michl, J. *J. Am. Chem. Soc.* **1992**, *114*, 6301. (d) Plitt, H. S.; Michl, J. *J. Chem. Phys. Lett.* **1992**, *198*, 400. (e) Plitt, H. S.; Balaji, V.; Michl, J. *J. Chem. Phys. Lett.* **1993**, *213*, 158. (f) Plitt, H. S.; Downing, J. W.; Raymond, M. K. Balaji, V.; Michl, J. *J. Chem. Soc., Faraday Trans.* **1994**, *90*, 1653.

Scheme 1



methyloligosilanes including the temperature dependence of their absorption and emission spectra. More recently, Kaito and co-workers reported the X-ray analysis, low-wavenumber Raman scattering, and liquid crystalline properties of films of permethyloligosilanes prepared by a vacuum-deposition method.⁸ Whereas the thermochromic behavior of polysilanes is known to depend significantly on the side-chain alkyl substituents, there has been reported no study of oligosilanes having long-chain alkyl substituents.⁹ We report here the synthesis and characterization of a series of perhexyloligosilanes and the unique temperature dependence of their absorption and emission spectra.

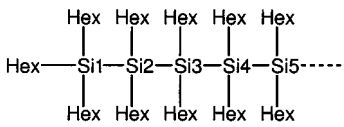
Results and Discussion

1. Synthesis and Characterization. A mixture of perhexyloligosilanes (**3a–10a**) was prepared by the Wurtz coupling of a mixture of trihexylchlorosilane and dihexyldichlorosilane with lithium in THF, as shown in Scheme 1. These perhexyloligosilanes were separated by recycle gel-permeation chromatography and characterized by means of ¹H, ¹³C, and ²⁹Si NMR spectroscopies, elemental analyses, and mass spectrometry. Permethyloligosilanes (**3b–10b**) as references were prepared by a similar procedure.⁷

²⁹Si NMR chemical shifts of a series of perhexyloligosilanes are summarized in Table 1. The number of signals and their relative intensities correspond to the number of Si units in each oligosilane. Signals appearing at the lowest and highest magnetic fields are assigned to the ²⁹Si nuclei of the terminal trihexylsilyl (Si1) and the next dihexylsilylene units (Si2), respectively. The ²⁹Si resonances of inner silylene units approach ca. –25 ppm, which is the value for high molecular weight poly(dihexylsilylene).¹⁰

The ²⁹Si NMR spectra of a series of permethyloligosilanes were studied by Kumada et al.^{11a} and West et

Table 1. ²⁹Si Chemical Shifts (ppm) of Perhexyloligosilanes in CDCl₃ at Room Temperature

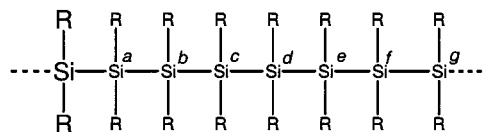


oligosilane	chemical shift/ppm				
	Si1	Si2	Si3	Si4	Si5
3a	-11.0	-41.0			
4a	-10.3	-34.9			
5a	-10.3	-34.6	-30.5		
6a	-10.2	-34.3	-28.9		
7a	-10.1	-34.0	-28.3	-27.0	
8a	-10.2	-33.9	-28.1	-26.6	
9a	-10.1	-33.8	-27.9	-26.3	-26.1
10a	-10.1	-33.8	-27.9	-26.2	-25.8

al.^{11b} in detail. The chemical shift of the *k*th silicon atom is known to be represented by eq 1

$$\delta_{Di(k)} = B + \sum_j A_j n_{kj} \quad (1)$$

where *A_j* is the chemical shift parameter for the *j*th atom from the *k*th silicon atom, *n_{kj}* is the number of those atoms present at that position, and *B* is a constant. The same equation is applicable to a series of perhexyloligosilanes with the following parameters (the corresponding values for permethyloligosilanes^{11b} are in parentheses):



B = +7.2 (+8.5), *a* = –24.1 (–28.5), *b* = +5.6 (+3.9), *c* = +1.1 (+1.2), *d* = +0.3 (+0.2), *e* = +0.3, *f* = +0.1, and *g* = +0.1 ppm. The ²⁹Si resonances for dihexylsilylene units in general appear at higher magnetic fields than those of dimethylsilylene units.

¹³C NMR spectroscopy is also useful to identify perhexyloligosilanes with a Si chain length shorter than nine.¹² All signals are classified into six groups due to six carbons of a hexyl group and assigned reasonably on the basis of their relative intensities and the assignment for poly(dihexylsilylene) reported by Schilling, Bovey, and Zeigler.¹⁰ It is noted that the resonances of C2 at the terminal silicons appear at 2.2–2.5 ppm higher fields than those for C2 at inner silicons, while resonances for C1 and C3–C6 appear in rather narrow regions. ¹³C resonances due to terminal methyl groups (C6) are overlapped and appear at around 14.1 ppm as an apparent sharp singlet. For octasilane (**8a**) and shorter oligosilanes (**3a–7a**), C1 resonances appear independently from each other and, therefore, are helpful in determining the Si chain-length.

There are three sets of signals, which are assigned to α-methylenes (0.6–0.8 ppm), terminal methyls (0.8–1.0 ppm), and β- to ε-methylenes (1.2–1.4 ppm), in the

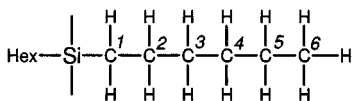
(8) (a) Yatabe, T.; Shimomura, M.; Kaito, A. *Chem. Lett.* **1996**, 551. (b) Shimomura, M.; Yatabe, T.; Kaito, A.; Tanabe, Y. *Macromolecules* **1997**, *30*, 5570. (c) Yatabe, T.; Kaito, A.; Tanabe, Y. *Chem. Lett.* **1997**, 799.

(9) In preliminary communications, we have studied perhexyl- and perpropyldecalanes and several propyl-substituted oligosilanes having terminal chiral aralkyl substituents: (a) Obata, K.; Kira, M. *J. Chem. Soc., Chem. Commun.* **1998**, 1309. (b) Obata, K.; Kabuto, C.; Kira, M. *J. Am. Chem. Soc.* **1997**, *119*, 11345.

(10) Schilling, F. C.; Bovey, F. A.; Zeigler, J. M. *Macromolecules* **1986**, *19*, 2309.

(11) (a) Ishikawa, M.; Iyoda, J.; Ikeda, H.; Kotate, K.; Hashimoto, T.; Kumada, M. *J. Am. Chem. Soc.* **1981**, *103*, 4845. (b) Stanislawsky, D. A.; West, R. *J. Organomet. Chem.* **1981**, *204*, 295.

(12) The ¹³C NMR data are given in the Supporting Information.



^1H NMR spectra of perhexyloligosilanes. The ^1H resonances due to α -methylenes of inner silicon atoms are found at lower fields to approach the region for terminal methyls.

Molecular weights of **3a**–**7a** were determined by mass spectrometry using EI ionization.

2. Absorption Spectra. Absorption spectral data of perhexyl- and permethyloligosilanes at 77 and 293 K are summarized in Table 2.

The band maxima and the absorption coefficients for the $\sigma \rightarrow \sigma^*$ transitions of perhexyloligosilanes having 3–10 Si atoms in the main chains are parallel to those of the corresponding permethyloligosilanes as shown in Table 2. Larger λ_{max} values for perhexyloligosilanes in comparison to those of the corresponding permethyloligosilanes at both 293 and 77 K may be ascribed mainly to the greater steric bulk of hexyl vs methyl substituents (*vide infra*).

The absorption spectra of these perhexyl- and permethyloligosilanes are temperature dependent, but the behavior is very different for short oligosilanes with 3–5 silicons (**3**–**5**) and long oligosilanes with 6–10 silicons (**6**–**10**). The former show significant blue shifts of the absorption bands with decreasing temperatures, while the latter show remarkable red shifts, as expected from the all-trans-like main-chain conformations favored at low temperatures.

2.1. Temperature Dependence of the Absorption Spectra of Short-Chain Oligosilanes. Short-chain oligosilanes **3a**–**5a** as well as **3b**–**5b** showed remarkable blue shifts with decreasing temperatures. As a typical example, the temperature dependence for **3a** is shown in Figure 1. Since the blue shifts are observed even in the trisilanes, the origin cannot be ascribed to the conformational change of the Si backbone. The following should be taken into account as the possible reasons for the temperature dependence observed for peralkyltrisilanes: (i) The relative importance of three rotational conformers around the Si–Si bonds (**A**–**C** in Figure 2a) depending on temperatures may contribute to the temperature-dependent absorption spectra. (ii) The transition energy of a trisilane may be modified by the temperature-dependent vibrational amplitudes of the three vibrational modes, two stretching and one bending modes (Figure 2b). These possibilities are inspected by *ab initio* MO calculations using GAUSSIAN 94 programs.¹³

Since among conformations **A**, **B**, and **C** no energy minimum was found for **B** and **C** at the HF/6-31G** level and since the $\sigma \rightarrow \sigma^*$ transition energies are not expected to differ significantly among these isomers, the temperature dependence of the distribution of these rotational conformations may be eliminated as the reason for the blue shift.

Table 2. UV Absorption Spectra of Perhexyl- and Permethyloligosilanes in 3-Methylpentane

oligo-silane	293 K			77 K		
	$\lambda_{\text{max}}/\text{nm}$	$\epsilon \times 10^4$	half-bandwidth/ 10^3 cm^{-1}	$\lambda_{\text{max}}/\text{nm}$	$\epsilon \times 10^4$	half-bandwidth/ 10^3 cm^{-1}
3a	217	1.2	<i>a</i>	211	2.2	<i>a</i>
4a	237	2.1	3.3	233	3.6	2.6
5a	250	2.6	3.4	250	5.9	2.2
6a	265	3.4	3.9	270	9.3	1.6
7a	274	3.8	3.9	283	11.0	1.6
8a	281	4.2	4.1	294	16.1	1.5
9a	286	4.5	4.5	302	20.3	1.3
10a	290	5.5	4.5	309	17.5	1.3
3b	217	1.1	<i>a</i>	211	2.1	<i>a</i>
4b	233	1.6	3.0	230	3.6	2.2
5b	250	1.9	3.3	250	5.5	1.9
6b	260	2.3	3.6	265	6.8	1.8
7b	269	2.9	<i>b</i>	274	9.5	1.7
8b	276	3.0	5.1	282	13.4	1.4
9b	278	4.4	<i>b</i>	288	15.4	1.7
10b	284	4.6	4.6	294	16.0	1.4

^a Shoulder. ^b A structured band.

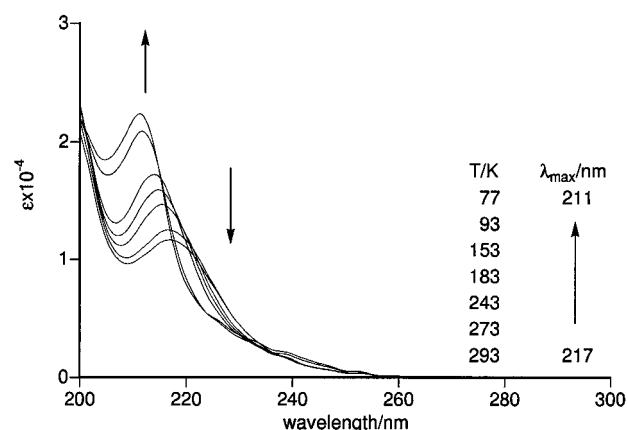


Figure 1. Temperature-dependent UV absorption spectra of **3a** (2.57×10^{-4} M) in 3-methylpentane.

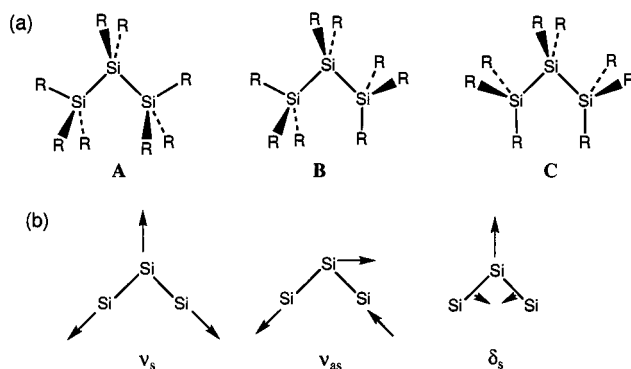


Figure 2. (a) Three rotational conformations of peralkyltrisilanes and (b) three vibrational modes of the trisilane skeleton.

Dependence of the $\sigma \rightarrow \sigma^*$ transition energy of the trisilane backbone on three vibrational modes of the trisilane skeleton, a symmetric stretching (ν_s), an anti-symmetric stretching (ν_{as}), and a bending (δ_s), was investigated as follows: With increasing temperatures, the vibrational amplitudes of these modes become larger and influence the absorption band maxima. To test how the transition energies of octamethyltrisilane are influenced by the Si–Si bond length and SiSiSi bond angle, CIS calculations were performed.

(13) Frish, M. J.; Truck, G. W.; Head-Gordon, M.; Gill, P. M. W.; Wong, W.; Foresman, J. B.; Johnson, B. G.; Schlegel, H. B.; Robb, M. A.; Repolgle, E. S.; Gompers, M.; Andrews, J. A.; Ragchavachari, K.; Binkley, J. S.; Gonzalez, C.; Martin, R. L.; Fox, D. J.; Defees, J.; Baker, J.; Stewart, J. P.; Pople, J. A. *GAUSSIAN 94*; Gaussian Inc.: Pittsburgh, PA, 1994.

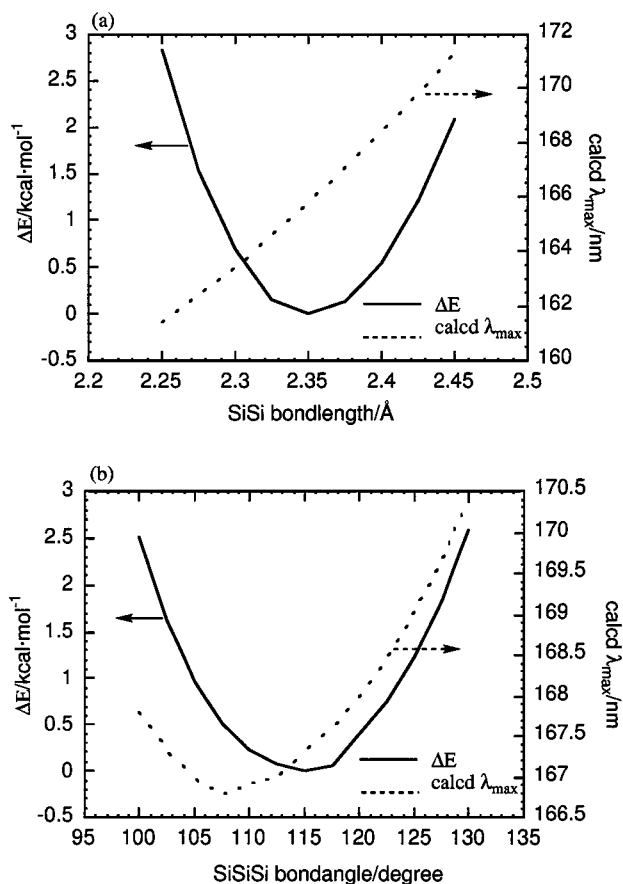


Figure 3. Plots of total energies (—) calculated at the B3P86/6-31G** level and absorption band maxima (···) calculated by the CIS/6-31G* method of **3b** vs (a) SiSi bond lengths and (b) SiSiSi bond angles.

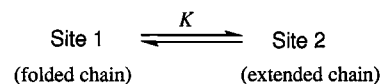
Stretching and bending potentials of octamethyltrisilane were calculated by varying the Si–Si bond length and SiSiSi bond angle, respectively, at the HF/6-31G** level; at each fixed geometry of the SiSiSi skeleton, the other degrees of freedom were relaxed. At each structure of the trisilane, total energy and absorption maximum were calculated at the B3P86/6-31G** and CIS/6-31G**//6-31G** levels, respectively. Figure 3a,b shows the bond length and bond angle dependence of the total energies and absorption maxima near the fully optimized geometry. The total energies are both nearly harmonic as functions of the bond length and bond angle near the equilibrium geometry. Since the calculated absorption maxima depend almost linearly on the bond length as expected (Figure 3a), the reduction of the stretching amplitude at lower temperatures will cause narrowing of the bandwidth but no shift of the band maximum. On the other hand, parabolic dependence of the absorption maxima on the bond angle as shown in Figure 3b will cause an increase of the average transition energy with decrease of the bending amplitude. The blue shift of the absorption maxima of the short-chain oligosilanes with decreasing temperatures will be explained qualitatively by the parabolic dependence of the absorption maximum on the bending angle. The parabolic dependence will be the consequence of the switching of the lowest energy transition from the HOMO–LUMO transition at wider bond angles than 112.5° to the HOMO–NLUMO (the second LUMO) transition at the narrower

bond angles; Michl et al. have found a similar tendency for the transitions of Si₃H₈ by the CISD/DZ calculations.^{7a}

2.2. Temperature Dependence of Absorption Spectra of Long-Chain Oligosilanes. The effects of the bending amplitude become less important for the longer chain oligosilanes and are overwhelmed by the red shift due to the ordering of the Si main chain from a random coil to a loose helical all-trans conformation. Absorption spectra of **6a–10a** and **6b–10b** show a continuous red shift with decreasing temperatures, which becomes larger as the length of the oligosilane chain increases. There are some differences to be noted between the spectra of permethyl- and perhexyloligosilanes. The absorption spectra of perhexyloligosilanes are rather sharp and structureless at low temperatures, while permethyloligosilanes show broad bands with fine structures in their spectra. The λ_{max} values of perhexyloligosilanes were 5–15 nm larger than those of the corresponding permethyloligosilanes at low temperatures. The long-chain perhexyloligosilanes show a stronger temperature dependence, similar to that of perhexylpolysilane polymers, suggesting that the barrier of the transition from the folded to extended chains is much larger than that for permethyloligosilanes, due to the steric effects of the side-chain alkyl substituents.

It is suggested that there is significant conformational disorder in permethyloligosilanes even at low temperatures, due to the lower rotational barriers around Si–Si bonds than those for the perhexyloligosilanes.

2.3. Effects of Side-Chain Alkyl Substituents on Thermochromic Behavior of Peralkyldecasilanes. As shown in a previous paper,^{9a} the absorption maxima of perhexyl- (**10a**), permethyl- (**10b**), and perpropyldecasilanes (**10c**) red-shift with decreasing temperatures. The extent of the red shift (Δλ_{max}) from 293 to 77 K is markedly dependent on the substituents; Δλ_{max} values are <19, 10, and 13 nm for **10a**, **10b**, and **10c**, respectively; with increasing chain length of the alkyl substituents, the thermochromic behavior of decasilanes more resembles that of poly(dihexylsilylene). The temperature dependence of the absorption spectrum of **10a** is analyzed by a two-site model similar to the transition from random coil to all-pseudo-trans rod model for poly(dihexylsilylene); site 1 (extended chain) with all-pseudo-trans rod conformations is more favored than site 2 (folded chain) with at least one gauche arrangement in the seven Si tetrads of **10a** at low temperatures.



The spectra of **10a** observed between 213 and 153 K are deconvoluted to the two different bands responsible for site 1 and site 2, which are represented by skewed Gaussian functions (eq 2).¹⁴

$$Y = Y_0 \exp[-\ln 2 \{ \ln(1 + 2b(X - X_0/\Delta X_{1/2})/b)^2 \}] \quad (2)$$

$$A = (\pi/\ln 2)^{1/2} Y_0 \Delta X_{1/2} \exp(b^2/4 \ln 2)/2 \quad (3)$$

where X is the wavenumber (cm⁻¹); X_0 , peak position

(14) Fraser, R. D. B.; Suzuki, E. *Anal. Chem.* **1969**, *41*, 37.2.

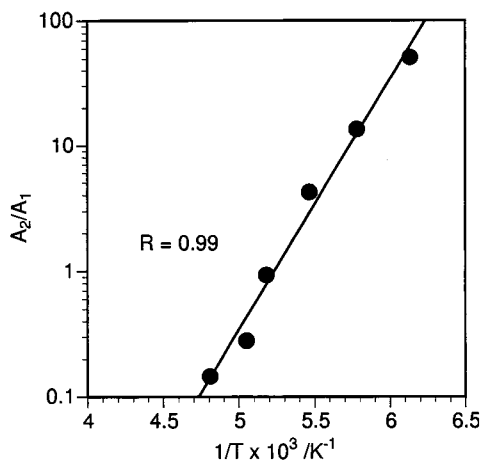


Figure 4. Plot of A_2/A_1 vs $1/T$ of **10a** in 3-methylpentane; A_1 and A_2 are areas of the absorption band for site 1 and site 2, respectively.

(cm^{-1}); Y_0 , heights; b ($\neq 0$), asymmetry factor, of the Gaussian function. Intensities of the two bands are estimated as the band areas (A_1 and A_2 for sites 1 and 2, respectively) calculated using eq 3. As shown in Figure 4, a good linear relationship is found between $\log(A_2/A_1)$ vs $1/T$; the enthalpy difference between the two sites is estimated to be -9.2 kcal/mol from the slope of the line.

The remarkable effect of the substituents on the temperature dependence of the absorption spectrum of decasilane is ascribed to the importance of the steric energies between the side-chain alkyl substituents. MM2 force field calculations using standard parameters for organosilicon compounds proposed by Allinger et al.¹⁵ showed that the energy differences between the extended and the folded conformations with one gauche turn in the 7 Si tetrads of a decasilane were ca. -8.9 and -5.3 kcal/mol for **10a** and **10c**, respectively, while the value was much smaller for **10b** (-0.5 kcal/mol). A one-gauche conformation in **10a** or **10c** causes severe steric repulsion between alkyl substituents, while the repulsion is less important in **10b**. The steric energy calculated by the MM2 method is in good accord with the experimental enthalpy differences for the transition from site 1 to site 2, suggesting that the transition occurs between an assembly of the folded chains with one or more gauche Si tetrads and an assembly of extended chains with all-pseudo-trans rod conformations.

3. Fluorescence Spectra. Fluorescence band maxima of perhexyloligosilanes as well as those of permethyloligosilanes measured in our laboratory are shown in Table 3. As first noted by Michl et al. for permethyloligosilanes,^{7e} emission spectra of these peralkyloligosilanes show interesting chain-length dependence. The emission behaviors are classified as four types: (i) no emission is observed for **3a** and **3b**^{7e} (and **4b**)¹⁶ (class 1), (ii) broad emission bands with large Stokes shifts are observed for **4a**, **5a**, **5b**, **6a**, and **6b** (class 2), (iii) sharp emission bands with small Stokes shifts are found for **9b**, **10a**,

Table 3. Emission Spectra of Perhexyloligosilanes in 3-Methylpentane^a

oligo-silane	293 K		77 K	
	λ_{em}/nm	Stokes shift/ 10^3 cm^{-1}	λ_{em}/nm	Stokes shift/ 10^3 cm^{-1}
4a	365 ^b	15	351	14
5a	375 ^c	12	343	9.9
6a	388	11	335	7.6
7a			297	1.8
8a	371 ^d	8.4	306	1.7
	321	3.2		
9a	370	7.6	309	0.9
	323	2.3		
10a	326	2.4	315	0.8
5b	371	13	364	9.9
6b	367 ^e	11	350	9.6
7b	295	2.4	285	1.5
	365	9		
8b	299	1.8	290	1.4
9b	303	1.8	299	1.4
10b	308	1.5	297	0.9

^a Excited at the absorption maxima. ^b At 123 K. ^c At 243 K. ^d At 273 K. ^e At 153 K.

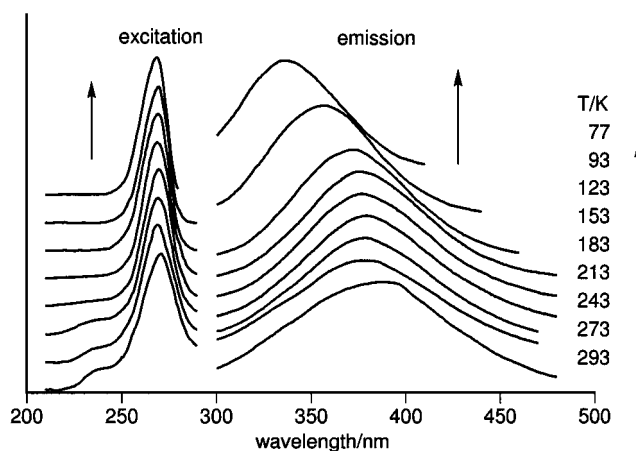


Figure 5. Temperature-dependent emission and excitation spectra of **6a** (8.2×10^{-6} M) in 3-methylpentane.

and **10b** (class 3), and (iv) the above two types of emission bands are observed simultaneously for **7a**, **7b**, **8a**, and **9a** with relative intensities depending on temperatures (class 4).

The broad emission bands with large Stokes shifts of **4a**, **5a**, and **6a** as well as **5b** and **6b** are weak and observed only at low temperatures. As a typical example, temperature-dependent emission and excitation spectra of **6a** are shown in Figure 5. The maxima blue-shift a little with decreasing temperature. Michl et al. have assigned the broad emission bands for short-chain oligosilanes to the emission from the "self-trapped exciton" exciton states, where an SiSi bond in the chain is stretched in the excited state and the exciton is trapped in the site.^{7,17}

Figure 6 shows temperature-dependent emission and excitation spectra of **10a** in 3-methylpentane. The sharp emission bands with small Stokes shift for class 3 oligosilanes are similar to those for poly(dihexylsilylene), and therefore, the bands are assigned to "free exciton" bands extended to the whole Si backbones.⁶

(15) Frierson, M. R.; Imam, M. R.; Zalkow, V. B.; Allinger, N. L. *J. Org. Chem.* **1988**, *53*, 5248.

(16) A broad emission band with a large Stokes shift has been observed for **4b** by Michl et al. probably using a fluorescence spectrophotometer with higher sensitivity.^{7e}

(17) Thorne, J. R. G.; Williams, S. A.; Hochstrasser, R. M.; Fagan, P. J. *Chem. Phys.* **1991**, *157*, 401.

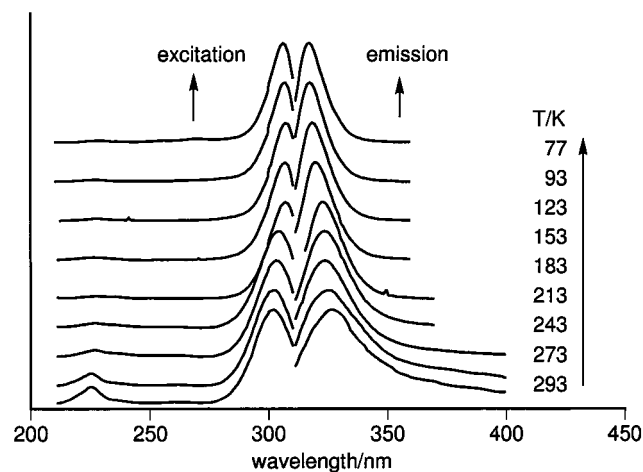


Figure 6. Temperature-dependent emission (excitation at 290 nm) and excitation (monitored at the emission maximum) spectra of **10a** (4.5×10^{-5} M) in 3-methylpentane.

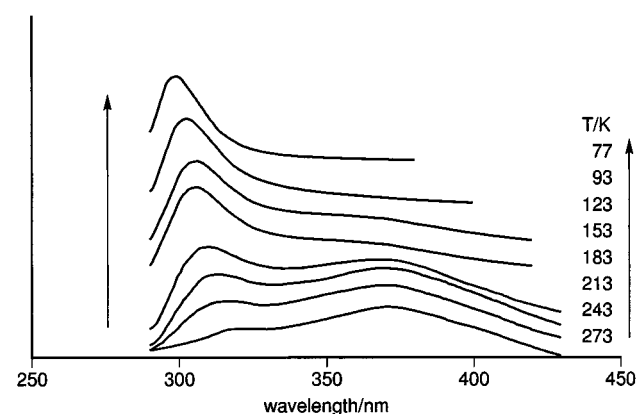


Figure 7. Temperature-dependent emission (excitation at 280 nm) spectra of **7a** (8.4×10^{-6} M) in 3-methylpentane.

The most interesting emission behavior is observed for class 4 oligosilanes. Emission spectra of **7a** are shown in Figure 7. At higher temperatures, **7a** shows both broad and sharp emission bands with larger intensity for the former emission. Since the excitation spectra of these two emission bands are both in good accord with the absorption spectra, they should have the same origin. Similar dual emission bands are observed for **7b**, **8a**, and **9a**, while the intensities of the broad emission bands decrease with increasing Si chain length. The intensity ratio of the broad to the sharp bands (I_b/I_s) of **7a** is much larger than that of **7b** at room temperature. However, the I_b/I_s for **7a** decreases rapidly and becomes smaller than that for **7b** at temperatures lower than 123 K. All these features are in good accord with the explanation given by Michl et al.^{7e} The significant alkyl-substituent effects on the I_b/I_s and their temperature dependence suggest that the self-trapped exciton may be formed selectively by the excitation of the folded conformations of heptasilanes, which are regarded as class 2 oligosilanes; as discussed in a previous section, the energy differences between the extended and the folded chains are much larger for hexyl-substituted oligosilanes than methyl-substituted oligosilanes. Further works will be required to obtain a detailed chemical view of the self-trapped excitation of the short oligosilanes.

Experimental Section

Apparatus. ^1H , ^{13}C , and ^{29}Si NMR spectra were recorded on a Varian Unity 300 FT-NMR spectrometer at 300, 75.4, and 59.6 MHz, respectively. Gas chromatography–mass spectra were recorded on a HP model 5971A mass spectrometer. Direct mass spectra were recorded on a HITACHI M-2500 mass spectrometer. Electronic absorption spectra were recorded on a Milton Roy Spectronic 3000 Array spectrometer. Emission and excitation spectra were recorded on a HITACHI 850 fluorescence spectrometer. For variable-temperature measurements, an OXFORD CF1204 cryostat was used. Gel permeation chromatography (GPC) was conducted by use of a LC-908 liquid chromatograph (Japan Analytical Instruments, Co. Ltd.) with JAIGEL-1H and -2H columns.

Materials. Dichlorosilane was supplied from Denki Kagaku Kogyo, Co. Ltd. Tetramethoxysilane, magnesium, acetyl chloride, $\text{H}_2\text{PtCl}_6 \cdot 6\text{H}_2\text{O}$, 1-hexene, lithium, and chloroform-*d* were commercially available. THF and Et_2O were dried over 4 Å molecular sieves for at least 1 day. Commercial 3-methylpentane was treated with concentrated sulfuric acid and distilled. Octamethyltrisilane (**3b**), decamethyltetrasilane (**4b**), dodecamethylpentasilane (**5b**), tetradecamethylhexasilane (**6b**), hexadecamethylheptasilane (**7b**), octadecamethyloctasilane (**8b**), icosamethylnonasilane (**9b**), and docosamethyldecasilane (**10b**) were synthesized by the reported procedure.⁷

Dihexyldichlorosilane (1).¹⁸ 1-Hexene (255 g, 4.0 mol) was added to a mixture of dichlorosilane (142 g, 1.4 mol) and $\text{H}_2\text{PtCl}_6 \cdot 6\text{H}_2\text{O}$ (10 mg, 0.019 mmol) with cooling by ice–water and stirred for 3 h. Compound **1** was separated by distillation as a colorless oil: bp 80 °C/0.5 mmHg; yield 196 g (0.73 mol, 52%); ^1H NMR (CDCl_3) δ 0.5–1.1 (m, 26 H); ^{13}C NMR (CDCl_3) δ 14.1, 16.2, 22.6, 23.0, 31.5, 32.9; MS m/z (rel intensity) 268 (M^+ , 3), 183 (100), 141 (58), 113 (32).

Trihexylchlorosilane (2).¹⁸ To a stirred solution of tetramethoxysilane (114 g, 0.75 mol) in 200 mL of diethyl ether was added 1.1 equiv of hexylmagnesium chloride in 500 mL of ether over a period of 2 h. The solution was refluxed for 3 h. The magnesium salts were removed by filtration. After evaporating the solvent, the reaction mixture was treated with acetyl chloride (294.5 g, 5.0 mol) at reflux for 4 h. Compound **2** was separated by distillation as a colorless oil: bp 115 °C/0.5 mmHg; yield 112 g (0.35 mol, 49%); ^1H NMR (CDCl_3) δ 0.6–1.9 (m, 39 H); ^{13}C NMR (CDCl_3) δ 14.1, 20.3, 22.3, 22.5, 31.3, 32.1; MS m/z (rel intensity) 318 (M^+ , trace), 233 (100), 149 (76), 107 (32).

Perhexyloligosilanes. A mixture of **1** (5.4 g, 20 mmol), **2** (3.2 g, 10 mmol), lithium powder (0.42 g, 60 mmol), and THF (70 mL) was placed into a two-necked 200 mL flask and stirred at reflux with a magnetic stirrer for 3 h. The reaction mixture was hydrolyzed with water. The organic layer was treated with a silica gel short column, and then the following oligosilanes were separated as pure substances by a recycle GPC. The yields are based on **2**. The purity of each oligosilane was analyzed by HPLC using a reverse-phase column. See the Supporting Information for a sample chromatogram.

Octahexyltrisilane (3a): a colorless oil; yield: 2.0%; ^1H NMR (CDCl_3) δ 0.6–0.8 (m, 16 H), 0.85–0.95 (m, 24 H), 1.2–1.5 (m, 64 H); ^{13}C NMR (CDCl_3) δ 12.2, 13.9, 14.2, 22.65, 22.70, 24.9, 26.9, 31.5, 31.6, 33.89, 33.93, several peaks are overlapped; ^{29}Si NMR (CDCl_3) δ -41.0, -11.0; MS m/z (rel intensity) 764 (M^+ , 45), 397 (100), 283 (98), 199 (97). Anal. Calcd for $\text{C}_{48}\text{H}_{104}\text{Si}_3$: C, 75.45; H, 13.69. Found: C, 75.30; H, 13.68.

Decahexyltetrasilane (4a): a colorless oil; yield: 2.6%; ^1H NMR (CDCl_3) δ 0.4–0.8 (m, 20 H), 0.85–0.95 (m, 30 H), 1.1–1.5 (m, 80 H); ^{13}C NMR (CDCl_3) δ 13.3, 14.1, 14.2, 22.7, 22.8, 25.0, 27.1, 31.57, 31.62, 33.90, 33.92, several peaks are

(18) Petrov, A. D.; Chernyshev, E. A. *Dokl. Akad. Nauk SSSR* **1952**, *86*, 737.

overlapped; ^{29}Si NMR (CDCl_3) δ -34.9, -10.3; MS m/z (rel intensity) 962 (M^+ , 27), 396 (20), 283 (39), 199 (100), 115 (78). Anal. Calcd for $\text{C}_{60}\text{H}_{130}\text{Si}_4$: C, 74.75; H, 13.59. Found: C, 75.13; H, 13.86.

Dodecahexylpentasilane (5a): a colorless oil; yield: 2.6%; ^1H NMR (CDCl_3) δ 0.6–0.7 (m, 12 H), 0.75–0.84 (m, 12 H), 0.9–1.0 (m, 36 H), 1.2–1.4 (m, 96 H); ^{13}C NMR (CDCl_3) δ 13.6, 14.1, 14.2, 14.3, 22.7, 22.8, 25.0, 27.1, 27.3, 31.60, 31.63, 31.7, 34.0, 34.1, 34.3, several peaks are overlapped; ^{29}Si NMR (CDCl_3) δ -34.7, -30.5, -10.3; MS m/z (rel intensity) 1160 (M^+ , 9), 793 (10), 679 (100), 595 (69), 396, (11), 283 (25), 199 (64), 115 (49). Anal. Calcd for $\text{C}_{72}\text{H}_{156}\text{Si}_5$: C, 74.39, H, 13.53. Found: C, 74.15; H, 13.57.

Tetradecahexylhexasilane (6a): a colorless and viscous oil; yield: 1.2%; ^1H NMR (CDCl_3) δ 0.6–0.7 (m, 12 H), 0.7–0.8 (m, 16 H), 0.8–0.9 (m, 42 H), 1.1–1.5 (m, 112 H); ^{13}C NMR (CDCl_3) δ 13.7, 14.1, 14.4, 14.5, 22.7, 22.8, 25.0, 27.1, 27.4, 31.60, 31.63, 31.8, 34.0, 34.1, 34.3, several peaks are overlapped; ^{29}Si NMR (CDCl_3) δ -34.28, -28.85, -10.21; MS m/z (rel intensity) 1358 (M^+ , 10), 1160 (2), 991 (8), 793 (47), 595 (35), 396 (29), 283 (46), 199 (100), 115 (87). Anal. Calcd for $\text{C}_{84}\text{H}_{182}\text{Si}_6$: C, 74.14, H, 13.48. Found: C, 74.29, H, 13.22.

Hexadecaheptylsilane (7a): a colorless and viscous oil; yield: 0.9%; ^1H NMR (CDCl_3) δ 0.6–0.7 (m, 12 H), 0.8–1.0 (m, 68 H), 1.2–1.4 (m, 128 H); ^{13}C NMR (CDCl_3) δ 13.8, 14.1, 14.4, 14.6, 14.8, 22.7, 22.8, 25.1, 27.2, 27.4, 27.5, 31.6, 31.81, 31.83, 34.0, 34.2, 34.4, several peaks are overlapped; ^{29}Si NMR (CDCl_3) δ -34.0, -28.3, -27.0, -10.1; MS m/z (rel intensity) 1556 (M^+ , 4), 1076 (7), 991 (25), 990 (23), 793 (20), 396 (52), 283 (29), 199 (100), 115 (91). Anal. Calcd for $\text{C}_{96}\text{H}_{208}\text{Si}_7$: C, 73.95, H, 13.45. Found: C, 73.56, H, 13.71.

Octadecaheptylsilane (8a): a colorless and viscous oil; yield: 0.7%; ^1H NMR (CDCl_3) δ 0.6–0.7 (m, 12 H), 0.8–1.0 (m, 78 H), 1.2–1.4 (m, 144 H); ^{13}C NMR (CDCl_3) δ 13.8, 14.1, 14.4, 14.6, 14.9, 22.7, 22.85, 22.87, 25.1, 27.2, 27.4, 27.5, 31.6, 31.81, 31.83, 34.0, 34.2, 34.38, 34.40, several peaks are overlapped; ^{29}Si NMR (CDCl_3) δ -33.9, -28.1, -26.6, -10.2. Anal. Calcd for $\text{C}_{108}\text{H}_{234}\text{Si}_8$: C, 74.14, H, 13.48. Found: C, 73.79, H, 13.58.

Eicosaheptylnonasilane (9a): a colorless and viscous oil; yield: 0.5%; ^1H NMR (CDCl_3) δ 0.6–0.8 (m, 12 H), 0.8–1.0 (m, 88 H), 1.2–1.4 (m, 160 H); ^{13}C NMR (CDCl_3) δ 13.8, 14.1, 14.4, 14.6, 14.9, 22.7, 22.85, 22.88, 25.1, 27.2, 27.4, 27.5, 31.6, 31.83, 31.87, 34.0, 34.2, 34.38, 34.41, several peaks are overlapped; ^{29}Si NMR (CDCl_3) δ -33.8, -27.9, -26.3, -26.1, -10.1.

Docosaheptyldecasilane (10a): a colorless and viscous oil; yield: 0.3% ^1H NMR (CDCl_3) δ 0.6–0.7 (m, 12 H), 0.8–1.0 (m, 98 H), 1.2–1.4 (m, 176 H); ^{13}C NMR (CDCl_3) δ 13.8, 14.1, 14.5, 14.7, 14.9, 15.0, 22.7, 22.8, 22.9, 25.1, 27.2, 27.4, 27.5, 31.6, 31.8, 31.9, 34.0, 34.2, 34.38, 34.40, several peaks are overlapped; ^{29}Si NMR (CDCl_3) δ -33.8, -27.9, -26.2, -25.8, -10.1. Anal. Calcd for $\text{C}_{132}\text{H}_{286}\text{Si}_{10}$: C, 73.56, H, 13.38. Found: C, 73.53, H, 13.50.

Supporting Information Available: ^{13}C NMR data of **3a–10a**, UV absorption data, and temperature-dependent UV and emission spectra of **3a–10a** and **3b–10b**, and temperature dependence of the relative intensities between broad and sharp emissions in **7a** and **7b**. This material is available free of charge via the Internet at <http://pubs.acs.org>.

OM990002W